Mon. Not. R. Astron. Soc. **399,** 744–749 (2009) doi:10.1111/j.1365-2966.2009.15174.x

The supergiant fast X-ray transient IGR J18483−0311 in quiescence: *XMM–Newton*, *Swift* and *Chandra* observations

A. Giunta,[1,2⋆] E. Bozzo,[1,3] F. Bernardini,[1,2] G. Israel,[1] L. Stella,[1] M. Falanga,[4] S. Campana,[5] A. Bazzano,[6] A. J. Dean[7] and M. Mendez[8]

[1]*INAF - Osservatorio Astronomico di Roma, Via Frascati 33, 00044 Rome, Italy*
[2]*Dipartimento di Fisica - Università di Roma Tor Vergata, via della Ricerca Scientifica 1, 00133 Rome, Italy*
[3]*ISDC, Geneva Observatory, University of Geneva, Chemin d'Ecogia 16, CH-1290 Versoix, Switzerland*
[4]*ISSI, Hallerstrasse 6, CH-3012 Bern, Switzerland*
[5]*INAF Osservatorio Astronomico di Brera, via Emilio Bianchi 46, I-23807 Merate (LC), Italy*
[6]*INAF - IASF, Via del Fosso del Cavaliere 100, 00133 Roma, Italy*
[7]*School of Physics and Astronomy, University of Southampton, Southampton SO17 1BJ*
[8]*Kapteyn Astronomical Institute, University of Groningen, PO Box 800, 9700 AV Groningen, the Netherlands*

Accepted 2009 May 30. Received 2009 May 29; in original form 2009 April 7

ABSTRACT

IGR J18483−0311 was discovered with *INTEGRAL* in 2003 and later classified as a supergiant fast X-ray transient. It was observed in outburst many times, but its quiescent state is still poorly known. Here, we present the results of *XMM–Newton*, *Swift* and *Chandra* observations of IGR J18483−0311. These data improved the X-ray position of the source, and provided new information on the timing and spectral properties of IGR J18483−0311 in quiescence. We report the detection of pulsations in the quiescent X-ray emission of this source, and give for the first time a measurement of the spin-period derivative of this source. In IGR J18483−0311, the measured spin-period derivative of $-(1.3 \pm 0.3) \times 10^{-9}$ s s^{-1} likely results from light travel time effects in the binary. We compare the most recent observational results of IGR J18483−0311 and SAX J1818.6−1703, the two supergiant fast X-ray transients for which a similar orbital period has been measured.

Key words: stars: individual: IGR J18483−0311 – stars: individual: SAX J1818.6−1703 – stars: neutron – X-rays: binaries – X-rays: stars.

1 INTRODUCTION

IGR J18483−0311 was discovered in 2003 during *INTEGRAL* deep observations of the Galactic Centre (Chernyakova et al. 2003). The mean source X-ray flux was ∼10 mCrab in the 15–40 keV, and ∼5 mCrab in the 40–100 keV band (Chernyakova et al. 2003; Molkov et al. 2004). The 18.5 d orbital period of the system was discovered by Levine & Corbet (2006) using *RXTE* archival data, and was later confirmed with *INTEGRAL* (Sguera et al. 2007). *INTEGRAL* data also showed that IGR J18483−0311 usually undergoes relatively long outbursts (∼3 d) that comprise several fast flares with typical time-scales of a few hours. During these bright events, the broad-band (3–50 keV) spectrum is best fit by an absorbed cut-off power-law model (photon index $\Gamma = 1.4$, cut-off energy $E_c = 22$ keV, and absorption column density $N_H = 9 \times 10^{22}$ cm^{-2}). Sguera et al. (2007) further detected a periodicity at 21.0526 ± 0.0005 s in the *INTEGRAL* data, and interpreted it as the spin-period of the neutron star (NS) hosted in IGR J18483−0311. The measured pulse fraction in the 4–20 keV energy band was 48 ± 7 per cent.[1] *Swift*/XRT observations in 2006 detected the source at a flux level of 4.2×10^{-12} erg cm^{-2} s^{-1} and provided a source position of $\alpha_{J2000} = 18^h48^m17\overset{s}{.}17$ and $\delta_{J2000} = -3^\circ10'15\overset{''}{.}54$ (estimated accuracy 3.3 arcsec, Sguera et al. 2007). This allowed Rahoui et al. (2008) to identify the optical counterpart of the X-ray source, a B0.5Ia star at a distance of 3–4 kpc, and to estimate its mass and radius ($M_* = 33\,M_\odot$ and $R_* = 33.8\,R_\odot$, respectively). These authors also suggested that an eccentricity $0.43 \lesssim e \lesssim 0.68$ could explain the 3-d duration of the outbursts (as reported by Sguera et al. 2007).

Based on these results, it was concluded that IGR J18483−0311 most likely belongs to the class of supergiant fast X-ray transients (SFXTs; Sguera et al. 2006, 2007; Walter & Zurita Heras 2007). However, due to the longer duration of its outbursts (a few days as opposed to a few hours) and a factor of ∼10 lower luminosity

⋆E-mail: giunta@oa-roma.inaf.it

[1] Here, we defined the pulsed fraction as $F = (I_{max} - I_{min})/(I_{max} + I_{min})$, where I_{max} and I_{min} are the measured count rates at the maximum and at the minimum of the folded light curve, respectively.

swings between outburst and quiescence, Rahoui et al. (2008) classified IGR J18483−0311 as an 'intermediate' SFXT, rather than a standard SFXT (see Walter & Zurita Heras 2007, for the definition of standard and intermediate SFXTs).

In this paper, we analyse a 18 ks *XMM–Newton* observation of IGR J18483−0311 in quiescence, and report the results of the spectral and timing analysis of this observation. We found that the pulse fraction of the source X-ray emission decreased significantly with respect to that measured while the source was in outburst, and provide for the first time an estimate of the spin-period derivative of this source. We also analysed all the available *Swift*/XRT observations of IGR J18483−0311, and studied the orbital variations of the source X-ray flux. A 1 ks *Chandra* observation is also analysed and provided an improved position of the X-ray source. The results from this study are then compared with those obtained recently on SAX J1818.6−1703, the other SFXT with a similar orbital period to that of IGR J18483−0311. So far, the orbital period has been measured with certainty only in other two SFXTs, that is IGR J16479−4514 (3.3194 d; Jain et al. 2009) and IGR J11215−5952 (Romano et al. 2007).[2]

2 IGR J18483−0311: DATA ANALYSIS AND RESULTS

2.1 *XMM–Newton* data

XMM–Newton (Jansen et al. 2001) observed IGR J18483−0311 on 2006 October 12, and the total good exposure time was 14.4 ks (we discarded observational intervals that were affected by a high background). The observation data files were processed to produce calibrated event lists using the standard *XMM–Newton* Science Analysis System (SAS 8.0). We used the EPPROC and EMPROC tasks for the EPIC-PN and the two MOS cameras, respectively. Source light curves and spectra were extracted in the 0.5–10 keV band, by using a circular extraction region with a radius of 20 arcsec. Background light curves and spectra were instead extracted by using a circular region with a radius of 50 arcsec. We used the SAS BACKSCALE task and the LCMATH task in HEASOFT (version 6.6.1) to account for the difference in extraction areas between source and background spectra and light curves, respectively. The times of all light curves were corrected to the barycentre of the Solar System with the SAS BARYCEN task. In all cases, owing to poor statistics, the EPIC-MOS1 and EPIC-MOS2 cameras did not contribute significant additional information on the source spectra. Therefore, in the following we discuss only the spectra from the EPIC-PN camera. All spectra were rebinned in order to have at least 25 photons for each energy bin.

In Fig. 1, we report the X-ray light curves of the source in the 0.5–5 and 5–10 keV energy bands; the lower panel of the figure shows the hardness ratio (i.e. the ratio of the count-rate in the hard, 5–10 keV, and soft, 0.5–5 keV, energy band) versus time. We note that the source count rate was decreasing during the first 5 ks of the observation. Unfortunately, the number of counts was insufficient to carry out any detailed investigation of the spectral variability. Therefore, we extracted only the 0.5–10 keV spectrum by using the total exposure time of the observation, and performed a fit with an absorbed power-law model. The best-fitting parameters were $N_{\rm H} = 7.7^{+1.2}_{-0.8} \times 10^{22}\,{\rm cm}^{-2}$, and $\Gamma = 2.5 \pm 0.3$ ($\chi^2_{\rm red}$/d.o.f. = 1.3/39; hereafter errors are at 90 per cent confidence level, unless otherwise indicated). The absorbed (unabsorbed) flux in the 0.5–10 keV band was $9.3 \times 10^{-13}\,{\rm erg\,cm^{-2}\,s^{-1}}$ ($5.2 \times 10^{-12}\,{\rm erg\,cm^{-2}\,s^{-1}}$). Assuming a source distance of 4 kpc, the unabsorbed flux corresponds to an X-ray luminosity (0.5–10 keV) of $1.0 \times 10^{34}\,{\rm erg\,s^{-1}}$. Fig. 2 shows the Epic-PN source spectrum, together with the best-fitting model and the residuals from this fit. The 90 per cent confidence upper limit to the equivalent width for narrow iron lines at 6.4 and 6.7 keV is 0.13 and 0.10 keV, respectively.

[2] However, note that the behaviour of IGR J11215−5952 is somewhat peculiar with respect to the other SFXTs, and thus Walter & Zurita Heras (2007) excluded this system from their SFXT source list.

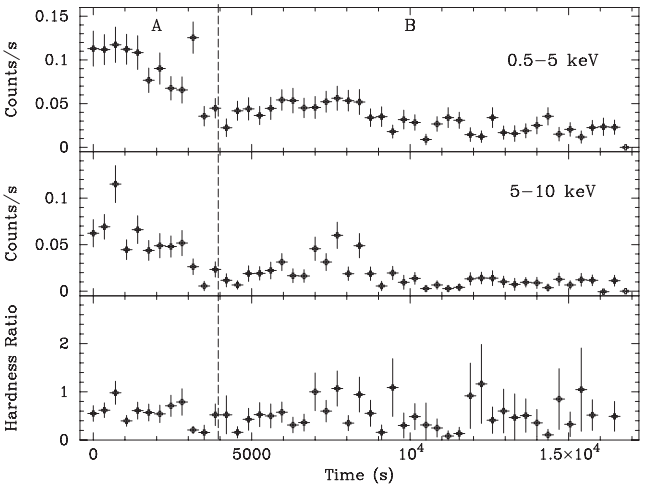

Figure 1. *XMM–Newton* Epic-pn light curve of IGR J18483−0311 in the two energy bands 0.5–5 and 5–10 keV (time bin is 350 s). The start time is 54020 (MJD) at 9:22:04. The lower panel of the figure shows the hardness ratio (i.e. the ratio of the count rate in the hard, 5–10 keV, and soft, 0.5–5 keV, energy band) versus time.

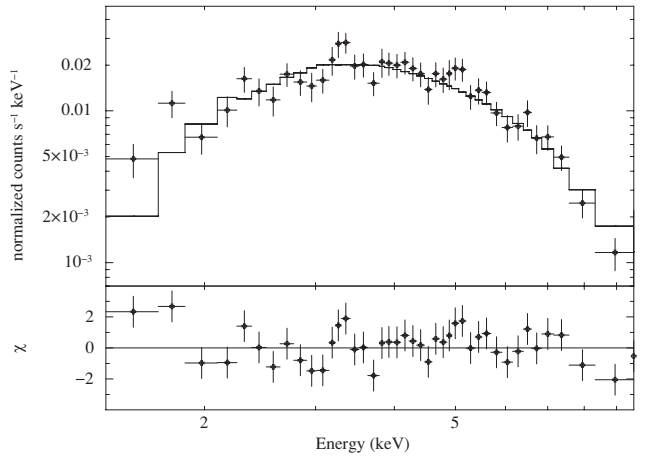

Figure 2. 0.5–10 keV *XMM–Newton* Epic-pn spectrum of IGR J18483−0311. The exposure time is 14.4 ks. The best fit is obtained using an absorbed power-law model (the best-fitting parameters are reported in the text). The lower panel of the figure shows the residuals from the best fit.

Timing analysis of the *XMM–Newton* data was carried out by using barycentred event files. We searched for the 21.0526 s spin-period of the NS in IGR J18483−0311 by performing first a power spectrum of the *XMM–Newton* data. No significant evidence for a peak at the corresponding frequency was found. In order to investigate further the presence of pulsations in the *XMM–Newton* data, we applied the Z^2_1-statistic technique (Buccheri 1988) to the photons event distribution for trial frequencies in a small window centred

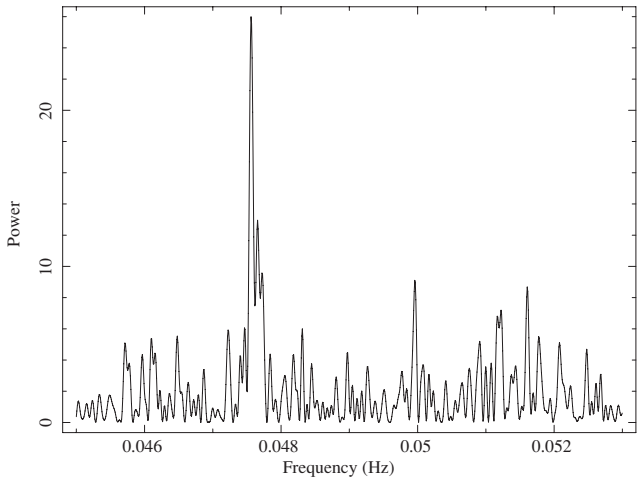

Figure 3. The Z_1^2-statistic power spectrum of IGR J18483−0311. We used the *XMM–Newton* Epic-pn event file in the 0.5–10 keV energy band. The peak at $Z_1^2 \sim 26$ corresponds to a spin-period of 21.025 ± 0.005 s.

on 0.0475 Hz (Sguera et al. 2007). A spin-period of 21.025 ± 0.005 s (hereafter errors on the NS spin periods are all at 1σ confidence level) is found with a peak power of $Z_1^2 \sim 26$. The single-trial significance of this period is 4.7σ. Fig. 3 shows the power spectrum computed with the Z_1^2-statistic technique by using the total exposure time of the *XMM–Newton* observation. This period estimate was then refined by employing a phase fitting technique (see e.g. Dall'osso et al. 2003). This gave our best-determined spin period of $P_{\rm spin} = 21.033 \pm 0.004$ s. In order to derive the significance of this result over the entire range of spin periods considered, we assumed a spin-period derivative of 1.3×10^{-9} s s^{-1} (see Section 4) and multiplied the single trial significance of the Z_1^2-statistic for the total number of trial $D_{\rm P}/(P_{\rm spin}^2/2Dt)$. Here $D_{\rm P}$ is the separation in seconds between our measured spin period and that reported by Sguera et al. (2007), and $Dt = 14.4$ ks is the total duration of the *XMM–Newton* observation. This gave us a significance of 3.7σ.

From the folded light curve of the observation (obtained with the EFOLD task, see Fig. 4), we measured a pulsed fraction of $F = 15 \pm 3$ per cent in the 0.5–10 keV energy band. The profile is consistent with a sinusoid. In order to investigate the energy dependence of the pulse fraction, we also extracted and folded light curves in different

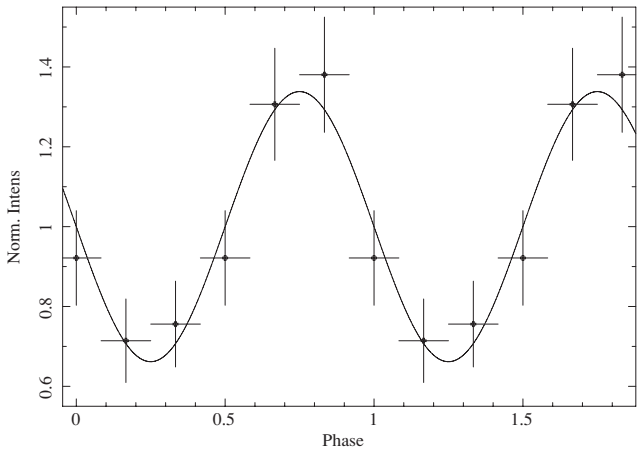

Figure 4. Results of the epoch-folding analysis on the 0.5–10 keV Epic-PN light curve of IGRJ18483−0311. We used the best-determined source spin-period $P_{\rm spin} = 21.033 \pm 0.004$ s.

Table 1. IGR J18483−0311 pulsed fractions (the time intervals 'A' and 'B' are indicated in Fig. 1).

Energy band	Total obs. (per cent)	A (per cent)	B (per cent)
0.5–10 keV	(15 ± 3)	$<29^a$	$<32^a$
0.5–5 keV	(23 ± 3)	(30 ± 5)	$<33^a$
5–10 keV	$<18^a$	$<36^a$	$<29^a$

[a] 3σ upper limit.

energy bands and time intervals. We found that the pulsed fraction decreases slightly towards higher energies, whereas no significant variation could be measured across the 'A' and 'B' time intervals shown in Fig. 1 (see Table 1). We note that the pulsed fraction, measured in the quiescent state of IGR J18483−0311, is a factor of ∼3 lower than that reported by Sguera et al. (2007) during the source outburst.[3]

2.2 *Swift* data

In Table 2, we show a log of the *Swift* observations analysed in the present study. Note that the observations ID 00035093001 and 00035093002 were also published previously by Sguera et al. (2007). We used the XRTPIPELINE (v.0.12.1) task to process *Swift*/XRT data (note that part of these data were published by Sguera et al. 2008). Standard event grades of 0–12 were selected for the XRT photon-counting (PC) mode; filtering and selection criteria were applied using FTOOLS (HEASOFT v.6.6.1). We created exposure maps through the XRTEXPOMAP task, and used the latest spectral redistribution matrices in the HEASARC calibration data base (v.011). Ancillary response files, accounting for different extraction regions, vignetting and point spread function corrections, were generated using the XRTMKARF task. When required, we corrected PC data for pile-up, and used the XRTLCCORR to account for this correction in the background subtracted light curves.

For each observation in Table 2, we extracted the light curve and spectrum, and derived a mean X-ray flux by fitting this spectrum with an absorbed power-law model (we used XSPEC v.12.5.0). Spectra were rebinned in order to have at least 20 photons per bin and allow for χ^2 fitting. In the observation ID. 00035093003, the very low source count rate ($8.6 \pm 2.7 \times 10^{-3}$) did not allow us for a detailed spectral analysis. Therefore, we estimated the source count rate of the observation with SOSTA (XIMAGE V.4.4.1), and then used this count rate within WEBPIMMS[4] in order to derive the X-ray flux (we assumed the same spectral model of the observation ID. 00035093002).

In Table 2, we report the best-fitting parameters obtained using an absorbed power-law model to characterize the source spectra; Fig. 5 shows the source light curves from the observations ID. 00035093001 and 00035093002 (note that, owing to poor statistics, we do not report the light curve of the observation ID. 00035093003).

2.3 *Chandra* data

Chandra observed IGR J18483−0311 on 2008 February 19 for a total exposure time of 1.2 ks with the High Resolution Camera. We

[3] However, note that these pulse fractions are measured in slightly different energy bands (see Section 1).
[4] http://heasarc.nasa.gov/Tools/w3pimms.html

Table 2. Log of the *Swift* observations of IGR J18483−0311 and SAX J1818.6−1703. Spectra are extracted for each observation in the table, and fit with an absorbed power-law model (absorption column density N_H and photon index Γ). F_{unabs} is the XRT/PC unabsorbed flux in the 0.5–10 keV energy band. EXP indicates the total exposure time of each observation (*Swift* observations comprise several snapshots and are not continuous pointings at the source).

Obs ID	Instr	Start time	Stop time	EXP (ks)	N_H (10^{22} cm^{-2})	Γ	F_{unabs} (erg cm^{-2} s^{-1})	χ^2_{red}/d.o.f.
IGR J18483−0311								
00035093001[c]	XRT/PC	2006-02-16 01:37:19	2006-02-16 22:36:57	7.9	$6.0^{+1.9}_{-1.6}$	$1.4^{+0.5}_{-0.4}$	5.3×10^{-11}	1.3/21
00035093002[c]	XRT/PC	2006-03-05 11:12:39	2006-03-05 17:58:56	5.6	5.0 ± 1.0	1.2 ± 0.3	6.4×10^{-11}	1.1/51
00035093003	XRT/PC	2008-09-26 13:49:39	2008-09-26 15:26:38	2.0	5.0 (fixed)	1.2 (fixed)	1.8×10^{-12}	—
SAX J1818.6−1703								
00036128001	XRT/PC	2007-11-09 17:47:09	2007-11-09 21:04:57	1.6	6.0 (fixed)	1.9 (fixed)	$<2.1 \times 10^{-12}$ [a,b]	—
00036128003	XRT/PC	2008-04-18 14:38:56	2008-04-18 17:45:49	2.0	6.0 (fixed)	1.9 (fixed)	3.5×10^{-12} [a]	—
00037889001	XRT/PC	2008-07-20 02:44:06	2008-07-21 01:21:56	3.7	6.0 (fixed)	1.9 (fixed)	8.5×10^{-12} [a]	—

[a] We determined the source count rate with sosta and used the spectral parameters given in in't Zand et al. (2006) within WEBPIMMS to estimate the source flux.
[b] 3σ upper limit.
[c] Previously reported by Sguera et al. (2007).

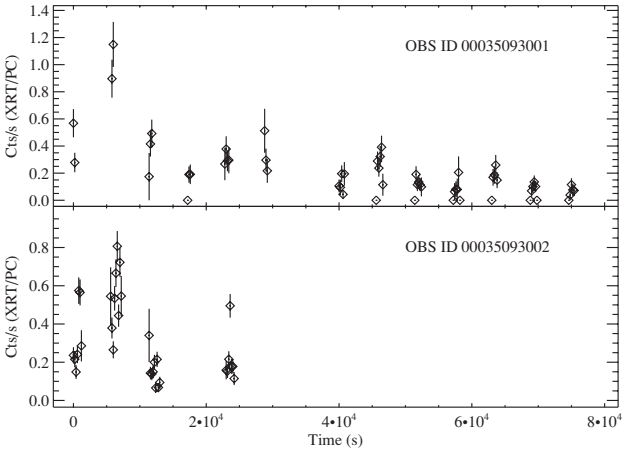

Figure 5. *Swift*/XRT light curves of the observations ID. 00035093001 (upper panel) and ID. 00035093002 (lower panel). The start times of the light curves in the upper and lower panel are 53782.0695 (MJD) and 53799.4690 (MJD), respectively.

reduced these data using the CIAO software (v 4.1.1) and the latest calibration file available. The best source position is provided by the WAVDETECT task at $\alpha_{J2000} = 18^h48^m17^s.2$ and $\delta_{J2000} = -3^\circ10'16''.8$ (the position accuracy is $0''.8$ at a 90 per cent confidence level). This is perfectly in agreement with the optical position reported by Rahoui et al. (2008). We also derived the source count rate (0.51 ± 0.02 cts s^{-1}) of the observation and then used this count rate with WEBPIMMS in order to estimate the source X-ray flux. The results are given in Table 3 (we assumed the same spectral model of the *XMM–Newton* observation).

3 SAX J1818.6−1703: DATA ANALYSIS AND RESULTS

3.1 *Swift* data

SAX J1818.6−1703 is the only SFXT with an orbital period comparable to that of IGR J18483−0311 (30 ± 0.1 d, Bird et al. 2009; Zurita-Heras & Chaty 2009). In Table 3, we report all observations of this source we found in the literature, together with two recent *Swift*/XRT observations that have not yet been published (ID. 00036128001 and 00037889001). We analysed all these *Swift*/XRT

Table 3. X-ray observations of IGR J18483−0311 and SAX J1818.6−1703 at different orbital phases.

IGR J18483−0311 Instrument	Phase	F_{unabs} [a] (erg cm^{-2} s^{-1})	L_X [c] (erg s^{-1})	Energy range
IBIS/ISGRI[1]	0	1.1×10^{-9}	2.1×10^{36}	20–100
SWIFT/XRT[10]	0.13	1.8×10^{-12}	3.5×10^{33}	0.5–10
Chandra/HRC[10]	0.24	4.3×10^{-10}	8.3×10^{35}	0.5–10
XMM/Epic-pn[10]	0.52	5.2×10^{-12}	1.0×10^{34}	0.5–10
SWIFT/XRT[10]	0.59	6.4×10^{-11}	1.2×10^{35}	0.5–10
SWIFT/XRT[10]	0.67	5.3×10^{-11}	1.0×10^{35}	0.5–10
SAX J1818.6−1703				
Instrument	Phase	F_{unabs} [a] (erg cm^{-2} s^{-1})	L_X [d] (erg s^{-1})	Energy Range
IBIS/ISGRI[2]	0	3.8×10^{-10}	2.9×10^{35}	18–60
IBIS/ISGRI[4]	0.01	3.0×10^{-9}	2.3×10^{36}	18–60
IBIS/ISGRI[5]	0.06	3.8×10^{-10}	2.9×10^{35}	18–60
SAX/WFC[6]	0.07	2.1×10^{-9}	1.6×10^{36}	2–9
SWIFT/XRT[10]	0.12	3.5×10^{-12}	2.6×10^{33}	0.5–10
SWIFT/XRT[10]	0.22	8.5×10^{-12}	6.4×10^{33}	0.5–10
XMM/Epic-pn[7]	0.51	$<1.1 \times 10^{-13}$ [b]	$<8.3 \times 10^{31}$ [b]	0.5–10
SWIFT/XRT[10]	0.76	$<2.1 \times 10^{-12}$ [b]	$<1.6 \times 10^{33}$ [b]	0.5–10
Chandra/ACIS-S[8,e]	0.89	7.5×10^{-12}	5.7×10^{33}	0.5–10
IBIS/ISGRI[3]	0.91	3.0×10^{-10}	2.3×10^{35}	18–45
IBIS/ISGRI+SWIFT/BAT[2]	0.98	$<3.8 \times 10^{-10}$ [b]	$<2.9 \times 10^{35}$ [b]	18–60
IBIS/ISGRI[2]	1.00	$<3.8 \times 10^{-10}$ [b]	$<2.9 \times 10^{35}$ [b]	18–60
IBIS/ISGRI+SWIFT/BAT[2]	1.00	9.1×10^{-10}	6.9×10^{35}	18–60
SWIFT/BAT[9]	1.00	2.2×10^{-9}	1.7×10^{36}	15–150

[a] Throughout this paper, we use the following conversion factors:
1 mCrab=2.08×10^{-11} erg cm^{-2} s^{-1} (2–10 keV)
1 mCrab=7.57×10^{-12} erg cm^{-2} s^{-1} (20–40 keV)
1 mCrab=9.42×10^{-12} erg cm^{-2} s^{-1} (40–100 keV).
[b] 3σ upper limit.
[c] From the unabsorbed flux and assuming a distance of 4 kpc (see Section 1).
[d] From the unabsorbed flux and assuming a distance of 2.5 kpc (Masetti et al. 2008).
[e] Not corrected for absorption.
References: (1) Sguera et al. (2007); (2) Bird et al. (2009); (3) Grebenev & Sunyaev (2008); (4) Grebenev & Sunyaev (2005); (5) Sguera et al. (2005); (6) in't Zand et al. (1998); (7) Bozzo et al. (2008c); (8) in't Zand et al. (2006); (9) Barthelmy et al. (2008, but see also http://gcn.gsfc.nasa.gov/notices_s/306379/BA/); (10) This work.

observations with the procedures described in Section 2.2 and reported the results in Table 2. Following Bird et al. (2009), we measured in Table 3 the orbital phase of each observation from the epoch of the outburst occurred on 53671 MJD (phase 0), so as to permit a comparison with the orbital changes of the X-ray flux in IGR J18483−0311. This comparison is carried out in Section 4.

4 DISCUSSION AND CONCLUSIONS

In this paper, we reported on all available quiescent observations of IGR J18483−0311, one of the two SFXTs for which the spin and orbital periods have been measured with certainty (the other is IGR J11215−5952 with $P_{\rm spin} = 186.78$ s, but see Section 1). We report the detection of pulsations in the quiescent X-ray emission of this source, and give for the first time a measurement of its spin-period derivative. To our knowledge, the spin-period has so far been detected unambiguously in two other SFXTs ($P_{\rm spin} = 228$ s, and 4.7 s in IGR J16465−4507 and IGR J1841.0−0536, respectively; Bamba et al. 2001; Walter & Zurita Heras 2007); however, the orbital period of these sources is not known. On the contrary, in the case of SAX J1818.6−1703 the orbital period is known, but the spin-period remains to be discovered.

Recently, it has been suggested that a measurement of the NS spin and orbital periods can be the key to distinguish between different models proposed for SFXT sources (Bozzo, Falanga & Stella 2008a). In fact, all these models involve a NS accreting from the intense wind of its supergiant companion, but several different mechanisms have been invoked in order to explain the very large luminosity swings observed during their transitions between outburst and quiescence (in't Zand 2005; Walter & Zurita Heras 2007). In particular, Bozzo et al. (2008a) suggested that, if very slow spinning NSs ($P_{\rm spin} \gtrsim 1000$ s) in relatively close orbits (few tens of days) are hosted in SFXTs, then a magnetic gating mechanism can be invoked in order to explain such luminosity swings. In this case, the NS magnetic field would be in the 'magnetar' range (i.e. $\gtrsim 10^{14}$–10^{15} G; Duncan & Thompson 1992). On the contrary, faster spin-periods might indicate that the large luminosity swings of SFXTs are caused by a centrifugal rather than a magnetic gating (a similar mechanism was suggested to explain the pronounced activity of Be X-ray pulsar transient systems; Stella, White & Rosner 1986). Alternatively, the observed variations in the X-ray luminosity of SFXTs might also be caused by drastic changes in the mass accretion rate on to the NS due to an extremely clumpy wind or to large-scale structure in the immediate surroundings of the supergiant companion. In these models, the orbital periods may be as high as hundreds of days (see, in particular, Sidoli et al. 2007; Negueruela et al. 2008).

In 2008, an *XMM–Newton* observation of IGR J16479−4514 revealed that also eclipse-like events can contribute to the luminosity swings observed in SFXTs (Bozzo et al. 2008b). Therefore, besides a measurement of the NS spin and orbital period, also an in-depth monitoring of the X-ray flux and spectral changes at different orbital phases is required in order to distinguish between different models or scenarios for SFXT sources.

To this aim, we presented in Table 3 an analysis of the orbital changes in the X-ray flux observed from IGR J18483−0311 and SAX J1818.6−1703, the only two SFXTs with a comparable orbital period. In the case of IGR J18483−0311, only few observations have been carried out in quiescence and thus the orbital monitoring of this source is far from being complete (following Sguera et al. 2007, we measured the source phases from the epoch of the brightest outburst observed with *INTEGRAL* at 53844.2 MJD). The lowest flux state of this source was caught by *Swift*/XRT at phase 0.13, that is relatively close to the orbital phase where the highest X-ray activity of the source has been observed in several occasions. Unfortunately, the poor statistics of this *Swift*/XRT observation prevented an accurate spectral analysis, and thus we could not investigate the origin of this low flux state. In the other two *Swift*/XRT observations, a spectral analysis could be carried out, but we did not detect any indication of a significant spectral variation. Only in the *XMM–Newton* observation, we measured a slight increase in the spectral power-law index. This suggests that X-ray flux changes in IGR J18483−0311 might have occurred due to genuine variations in the mass accretion rate on to the NS, rather than eclipse-like events. Note that, the detection of pulsations in the *XMM–Newton* data are also in agreement with the accretion scenario.[5] This suggests that SFXTs undergo low level accretion even when they are not in outburst (see also Sidoli et al. 2007).

At odds with the case of IGR J18483−0311, Table 3 shows that the different orbital phases of SAX J1818.6−1703 have been fairly well monitored. Unfortunately, the X-ray spectrum of this source could be well characterized only during the outburst, whereas in quiescence only the *Chandra* observation provided a measurement of the spectral parameters (see Table 2). In all the other observations only a rough estimate of the source flux could be obtained. Note that the source was not detected by *XMM–Newton* at the orbital phase 0.52, and the 3σ upper limit on the source X-ray flux was at least an order of magnitude lower than the fluxes measured in any other orbital phases. Since no spectral analysis could be carried out on SAX J1818.6−1703 at this orbital phase, the origin of this low flux event could not be investigated further. In case future observations of SAX J1818.6−1703 reveal that this source regularly undergoes X-ray eclipses at the orbital phase ∼0.5, this can help clarifying the issue of the extreme flux changes in this source.

More observations of IGR J18483−0311 and SAX J1818.6−1703 at different orbital phases with high sensitivity X-ray telescopes, like *XMM–Newton* and *Chandra*, are clearly required in order to understand unambiguously the origin of their outburst/quiescent activity. Being these two sources the only SFXTs with a comparable orbital period, they are very well suited to test different models proposed to explain the behaviour of SFXTs. We are currently investigating the results of the application of the gated accretion model to IGR J18483−0311 and SAX J1818.6−1703 (Bozzo et al., in preparation).

In this paper, besides X-ray flux changes, we also measured a spin-period variation in IGR J18483−0311. By using our best-determined spin period, $P_{\rm spin} = 21.033 \pm 0.004$ s, and that found previously by Sguera et al. (2007), we obtained a spin-period derivative in IGR J18483−0311 of $\dot{P}_{\rm spin} = -(1.3 \pm 0.3) \times 10^{-9}$ s s^{-1}. This value is comparable with the spin-period derivative measured in the case of the SFXT AX J1841.0−0535 (-1.5×10^{-10} s s^{-1} Sidoli et al. 2007) and those induced by accretion torques in wind-fed binaries (see e.g. Bildsten et al. 1997). However, in the present case, we believe that the spin-period derivative most likely results from light travel time effects in the binary. In fact, in a binary system with an orbital period of ∼18.5 d, these effects can contribute to an apparent spin-period derivative of the order of $\sim v_{\rm orb}/c = 8.6 \times 10^{-4}$ s s^{-1}, that is much larger than the spin-period derivative we reported above (here $v_{\rm orb}$ is the orbital velocity and c is the light velocity; we used the mass and radius of the supergiant companion

[5] Pulsations in quiescence were also reported for other two SFXT sources, that is IGR J16465−4507 (Walter et al. 2006) and AX J1841.0−0535 (Sidoli et al. 2007).

measured by Rahoui et al. 2008). Unfortunately, since a detailed orbital solution for this source is not yet available, we do not know if accretion torques acting on to the NS in IGR J18483−0311 might also have contributed to the observed spin-period derivative. Note that, in principle, this can be used to study the interaction between the NS and the inflowing matter from the supergiant companion (see e.g. Bozzo et al. 2008a).

An orbital monitoring of IGR J18483−0311 is required in order to understand the origin of the measured spin-period derivative.

ACKNOWLEDGMENTS

We thank the anonymous referee for his/her many helpful comments. EB thank M. Capalbi, M. Perri and K. Page for kind help with the *Swift*/XRT data analysis. This work was partially supported through ASI and MIUR grants.

REFERENCES

Bamba A., Yokogawa J., Ueno M., Koyama K., Yamauchi S., 2001, PASJ, 53, 1179
Barthelmy S. D., Krimm H. A., Markwardt C. B., Palmer D. M., Ukwatta T. N., 2008, GCN Circular, 7419, 1
Bildsten, et al., 1997, ApJS, 113, 367
Bird A. J. et al., 2009, MNRAS, 393, 11
Bozzo E., Falanga M., Stella L., 2008a, ApJ, 683, 1031
Bozzo E., Stella L., Israel G., Falanga M., Campana S., 2008b, MNRAS, 391, L108
Bozzo E. et al., 2008c, Astron. Telegram, 1493
Buccheri R., 1983, A&A, 128, 245
Chernyakova M., Lutovinov A., Capitanio F., Lund N., Gehrels N., 2003, Astron. Telegram, 157
Chetana J., Biswajit P., Anjan D., 2009, MNRAS, 393, L11
Dall'Osso S., Israel G. L., Stella L., Possenti A., Perozzi E., 2003, ApJ, 599, 485
Duncan R. C., Thompson C., 1992, ApJ, 392, L9
Grebenev S. A., Sunyaev R. A., 2005, Astron. Lett., 31, 672
Grebenev S. A., Sunyaev R. A., 2008, Astron. Telegram, 1482, 1
in 't Zand, 2005, A&A, 441, L1
in 't Zand J., Heise J., Smith M., Muller J. M., Ubertini P., Bazzano A., 1998, IAU Circ., 6840, 2
in't Zand J., Jonker P., Mendez M., Markwardt C., 2006, Astron. Telegram, 915
Jansen A., Lumb D., Altieri B. et al., 2001, A&A, 365, L1
Levine A. M., Corbet R., 2006, Astron. Telegram, 940
Masetti N. et al., 2008, A&A, 482, 113
Molkov S. V., Cherepashchuk A. M., Lutovinov A. A., Revnivtsev M. G., Postnov K. A., Sunyaev R. A., 2004, Astron. Lett., 30, 534
Negueruela I., Torrejon J. M., Reig P., Ribo M., Smith D. M., 2008, in Bandyopadhyay R. M., Wachter S., Gelino D., Gelino C. R., eds, AIP Conf. Ser. Vol. 1010, A Population Explosion: The Nature and Evolution of X-ray Binaries in Diverse Environments. Am. Inst. Phys., New York, p. 252
Rahoui F., Chaty S., Lagage P., Pantin E., 2008, A&A, 484, 801
Romano P. et al., 2007, Astron. Telegram, 1151
Sguera V. et al., 2005, A&A, 444, 221
Sguera V. et al., 2006, ApJ, 646, 452
Sguera V. et al., 2007, A&A, 467, 249
Sguera V. et al., 2008, A&A, 487, 619
Sidoli L. et al., 2007, A&A, 476, 1307
Sidoli L. et al., 2008, ApJ, 687, 1230
Stella L., White N. E., Rosner R., 1986, ApJ, 308, 669
Walter R., Zurita Heras J. A., 2007, A&A, 476, 335
Walter R. et al., 2006, A&A, 453, 133
Zurita Heras J. A., Chaty S., 2009, A&A, 493, L1

This paper has been typeset from a TEX/LATEX file prepared by the author.

